Catalysis Letters
https://doi.org/10.1007/s10562-022-04111-2

Perovskite Supported Catalysts for the Selective Oxidation of Glycerol to Tartronic Acid

Christopher D. Evans[1] · Jonathan K. Bartley[1] · Stuart H. Taylor[1] · Graham J. Hutchings[1] · Simon A. Kondrat[2]

Received: 21 April 2022 / Accepted: 9 July 2022

Abstract

Exceptional selectivity of $LaMnO_3$ perovskite supported Au catalysts for the oxidation of glycerol to the dicarboxylate tartronic acid is reported. Through using monometallic Au, Pt or bimetallic Au:Pt nanoparticles the tartronic acid yield could be altered significantly, with a maximum yield of 44% in 6 h with $Au/LaMnO_3$ and 80% within 24 h. These $LaMnO_3$ supported catalysts were compared with conventionally TiO_2 supported catalysts, which at comparable reaction conditions produced lactic acid, via a dehydration pathway, in high yield and a maximum tartronic acid yield of only 9% was observed. The $LaMnO_3$ catalysts produced minimal lactic acid regardless of the supported metal, showing that the support structure influences the prevalence of dehydration and oxidation pathways. The choice of metal nanoparticle influenced product selectivity along the oxidation pathway for both $LaMnO_3$ and TiO_2 supported catalysts. Au catalysts exhibited a higher selectivity to tartronic acid, whereas AuPt catalysts produced glyceric acid and Pt catalysts produced predominantly C–C scission products.

Graphical Abstract

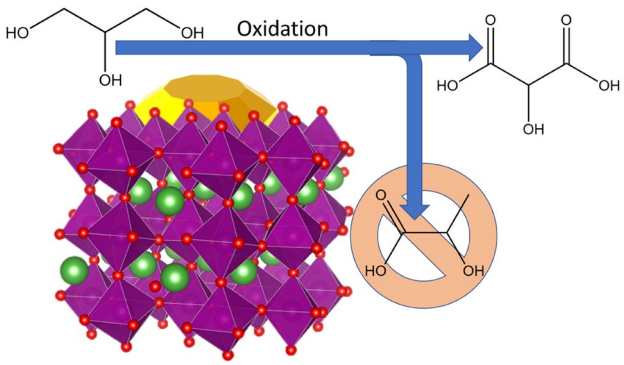

Keywords Glycerol oxidation · Dicarboxylic acid production · Perovskite supported catalyst

1 Introduction

The synthesis of carboxylic acids, from the aqueous oxidation of bio-derived polyols, such as glycerol, represents an important route to upgrading biomass to pharmaceuticals, polymers and fine chemicals [1, 2]. Ideally, for environmental and economic reasons, these transformations should be performed at low temperature, pressure and with the use of molecular oxygen as the oxidant.

The oxidation of glycerol, using noble metal catalysts (supported nanoparticles comprising Au, Pd, Pt and alloy

✉ Graham J. Hutchings
Hutch@Cardiff.ac.uk

✉ Simon A. Kondrat
S.Kondrat@lboro.ac.uk

[1] School of Chemistry, Cardiff Catalysis Institute, Cardiff University, Main Building, Park Place, Cardiff CF10 3AT, UK

[2] Department of Chemistry, Loughborough University, Loughborough, Leicestershire LE113TU, UK

Published online: 18 August 2022

combinations) [3–8], with and without the presence of bases [9, 10], is well reported in the scientific literature. Depending on the catalyst employed and reaction conditions used (T: 25–100 °C, P_{O2}: 1–10 bar, base: glycerol of 0–4:1) a range of different reaction products have been reported; from the initial oxidation products of glyceraldehlyde and dihydroxyacetone, to sequential oxidation C_3 carboxylic acid products (such as glyceric and tartronic acid), and also scission products (CO_2, C_2 and C_1 acids) [11]. In addition, under highly basic conditions and elevated temperatures (T: > 80 °C, glycerol:base 1:4), lactic acid can be produced via the dehydration of glyceraldehlyde to form pyruvaldehyde, which then undergoes a rearrangement to form lactic acid [12–15].

While most of these products can be attained in high yield, the selective formation of tartronic acid remains challenging. As a highly functional dicarboxylic acid, tartronic acid is considered a promising and versatile intermediate in polymer and pharmaceutical applications, and therefore is a highly desirable product from polyol oxidation [8]. Tartronic acid is formed by the further oxidation of glyceric acid, but frequently is observed as the minor product (selectivities < 20%) compared to glyceric acid [11].

Strategies for attaining high activity and good tartronic acid yields appear to be obvious; with greater catalytic activity and more aggressive oxidising conditions forcing the sequential oxidation of glyceric acid to tartronic acid. However, the limited number of papers reporting high tartronic acid yield suggests that this is in fact not easy to achieve. Firstly, highly active metals such as Pt or Pd, which can facilitate initial hydrogen abstraction from glycerol, unfortunately also enable scission reactions [4, 5, 11]. Supported Au catalysts have been shown to be highly selective for glycerol oxidation towards glyceric acid [4] and therefore, with a longer reaction, could perform the sequential oxidation to tartronic acid. Unfortunately, the activity of monometallic Au catalysts is low. Indeed, Cai *et. al.* demonstrated a high tartronic acid yield of 80% using a Au/HY zeolite catalyst but with a very low turn-over frequency (TOF) of 40 h^{-1} [16]. A method of improving the catalytic activity of Au has been to alloy with Pd or Pt but, while glycerol oxidation activity can be dramatically improved, selectivities towards tartronic acid remain low at the reaction conditions tested [6, 7, 17]. In an alternative strategy, Jin *et. al.* utilised a noble metal free Co/MgO-Al_2O_3 catalyst that produced a tartrtonic acid yield of 63.5%, but again with very low TOF of 3 h^{-1} [18].

In addition to catalyst design, reaction conditions such as increasing the base:glycerol ratio and elevating temperature enhances further oxidation. Both the Au/HY zeolite and Co/MgO-Al_2O_3 catalyst systems were run with high base:glycerol ratios of 4:1 and 7:1 respectively [16, 18]. Interestingly, the logical step of increasing reaction temperature, from the conventional 60–70 °C, to increase reaction rate was not employed in either study. The probable reason is that at > 80 °C the dehydration/rearrangement pathway of glyceraldehyde to lactic acid becomes viable [12, 13]. Therefore, at high temperature and base concentrations, tartronic acid formation is inhibited by these side reactions.

These side reactions can be mediated through choice of catalyst support [19–21]. Recently, it has been demonstrated that supporting AuPt onto high surface area lanthanum based perovskite supports ($LaBO_3$, where B was Cr, Mn, Fe, Co or Ni) allowed for control of the glycerol oxidation pathway [14, 22]. It was found that at operating conditions of 100 °C, 3 bar oxygen and a ratio 4:1 base to glycerol the dehydration/rearrangement pathway to lactic acid or oxidation pathway could be switched on or off by choice of perovskite B site element. The $LaMnO_3$ support, with its high reported oxygen adsorption capacity and activity for the oxygen reduction reaction, was found to inhibit the dehydration/rearrangement pathway and favour oxidation [23]. Here we report a systematic study to design a tartronic acid synthesis catalyst based on variation of the Au:Pt ratio while employing a $LaMnO_3$ support.

2 Experimental Method

2.1 Preparation of Perovskite Supports

Lanthanum manganite ($LaMnO_3$,) was prepared by supercritical CO_2 anti-solvent precipitation (SAS). This SAS process was chosen as it produces high surface area materials with low impurity content (such as alkali metals) and exceptional mixing of components [14, 24]. A summary of the preparation method is given below, with a more detailed experimental method described elsewhere [24]. A solution of lanthanum (III) acetylacetonate hydrate (4 mg ml^{-1}/Sigma Aldrich) and manganese (II) acetate tetrahydrate (2.7 mg ml^{-1}/Sigma Aldrich > 99.9% purity) in methanol (reagent grade, Fischer Scientific) was prepared. The metal salt solution was pumped at 4 ml min^{-1} (using an Agilent HPLC) through a coaxial nozzle, along with carbon dioxide (BOC) at 12 kg h^{-1}, into a vessel held at 130 bar and 40 °C. The resulting precipitate was recovered on a stainless steel frit; the CO_2-solvent mixture flowed down stream where the pressure was decreased to separate the solvent and CO_2. After 120 min the precipitation process was completed, the system was purged with CO_2 for 30 min at 130 bar and 40 °C. The system was then depressurised, and the dry powder collected. The SAS precipitate was then calcined at 750 °C in static air (ramp rate of 2 °C min^{-1}) for 4 h to form the perovskite.

2.2 Addition of Au/ Pt Nanoparticles to Perovskite Supports

Au, Pt and AuPt nanoparticles were deposited onto the perovskite supports using the sol-immobilisation procedure [14]. For the preparation of sols, aqueous solutions of $HAuCl_4$ (Johnson Matthey), $PdCl_2$ (Johnson Matthey) and $PtCl_2$ (Johnson Matthey) were prepared at the desired concentrations. Polyvinyl alcohol (PVA, 1 wt% aqueous solution, Aldrich, MW = 10 kDa) was freshly prepared and used as the stabilizer. NaBH4 (Sigma Aldrich, 0.1 M aqueous solution) was also freshly prepared and used as the reducing agent. To an aqueous mixture of $HAuCl_4$ and $PtCl_2$ of the desired concentration (1: 1 metal weight ratio, 1 wt% total metal in final catalyst) the PVA solution was added [PVA/(Au + Pt) (wt/wt) = 0.65] with vigorous stirring for 2 min. $NaBH_4$ was then added rapidly such that the $NaBH_4$: total metal ratio (mol/mol) was 7.5. The support perovskite was then added to the solution and after 1 h of stirring the mixture was filtered, washed with distilled water and dried at 120 °C for 16 h.

2.3 Catalyst Testing

Reactions were performed using a 50 mL Radleys glass reactor. The aqueous glycerol solution [0.3 M, containing NaOH (NaOH/glycerol ratio = 4, mol/mol)] was added into the reactor. The reactor was then heated to 80 °C prior to being purged three times with oxygen. Then the desired amount of catalyst (glycerol/metal ratio = 1000, mol/mol) was suspended in the solution and the reactor heated to 100 °C. The system was then pressurised to 3 bar O_2 and the reaction mixture stirred at 900 rpm. After the stated reaction time, the reactor vessel was cooled to room temperature and the reaction mixture diluted by a factor of 10 before being analysed by HPLC (Agilent 1260 infinity HPLC). The HPLC was equipped with ultraviolet and refractive index detectors and a Metacarb 67H column (held at 50 °C) to separate products. The eluent was an aqueous solution of H_3PO_4 (0.01 M), used at a flow rate of 0.8 ml min^{-1}. Quantification of reactants consumed and products generated was determined by an external calibration method. The reaction effluent was analysed for the following products; glyceric acid, tartronic acid, oxilic acid, glycolic acid and lactic acid.

3 Results

As previously reported in detail and summarised in Table 1, the SAS prepared $LaMnO_3$ comprised of 100% orthorhombic $LaMnO_3$ according to XRD, without evidence of single metal oxides, and with a surface area 32 m^2g^{-1}. The high purity and reasonable surface area allowed for the successful deposition of Au, AuPt or Pt onto the support. Representative TEM analysis (Figs. 1 and 2) showed that metal particle sizes of 2.1 nm (± 0.9 nm) where achieved on the $LaMnO_3$ support. In comparison, TiO_2 with a surface area of 61 m^2g^{-1} also allowed for the successful deposition of monometallic Au or Pt and bimetallic AuPt nanoparticles with a representative particle size of 1.7 nm (± 0.8 nm).

Table 1 Metal loading of AuPt catalysts and surface areas of supported catalysts

Sample	Au (molar %)	Pt (molar %)	Surface area (m^2g^{-1})
$AuPt/TiO_2$	52.75	48.15	61
AuPt/LaMnO3	50.50	49.50	32

The sequential oxidation of glycerol to glyceric acid and then onto tartronic acid requires relatively strong oxidising conditions, such as a high base to substrate ratio and elevated temperatures; in this study a NaOH:glycerol ratio of 4:1 was used with a reaction temperature of 100 °C. As previously mentioned, while this will push sequential oxidation reactions it will also facilitate dehydration and rearrangement reactions [13].

Initially, the effect of metal composition with a conventional TiO_2 support, on product distribution was investigated. As observed from time-on line data in Fig. 3 and Table 2, irrespective of the use of Au, Pt or AuPt nanoparticles, TiO_2 supported catalysts all had a high selectivity, of *ca.* 70%, towards lactic acid (the product of glyceraldehyde dehydration and rearrangement). The activity of the Pt catalyst was higher than Au with a TOF of 350 h^{-1} vs 220 h^{-1} respectively, however a significantly higher C–C scission was seen with Pt as the reaction progressed. These observations, regarding oxidation pathway, are comparable to previously reported studies at lower temperatures of 60 °C [19]. The $AuPt/TiO_2$ catalyst retained the activity of the Pt/TiO_2 with a TOF of 320 h^{-1} but with significantly lower C–C scission selectivity and higher glyceric acid selectivity. Despite the ability of Au to mediate C–C scission, as a monometallic catalyst or as part of a AuPt alloy, the dominance of the dehydration pathway resulted in poor tartronic acid yield (below 10% after 6 h time online) regardless of metal combination. Another interesting observation was that the rate of glycerol conversion significant dropped after 2 h time online with the Au/TiO_2 catalyst, with conversion increasing from 36 to 42% from 2 to 6 h (this 6% representing a 22% growth in conversion). By comparison conversion increased from 55 to 81% (47% growth) over the same time period with $AuPt/TiO_2$. This result suggest that the Au/TiO_2 catalyst deactivates over the reaction time period, relative to Pt containing catalysts. Lui and co-workers noted the same phenomenon, with Au

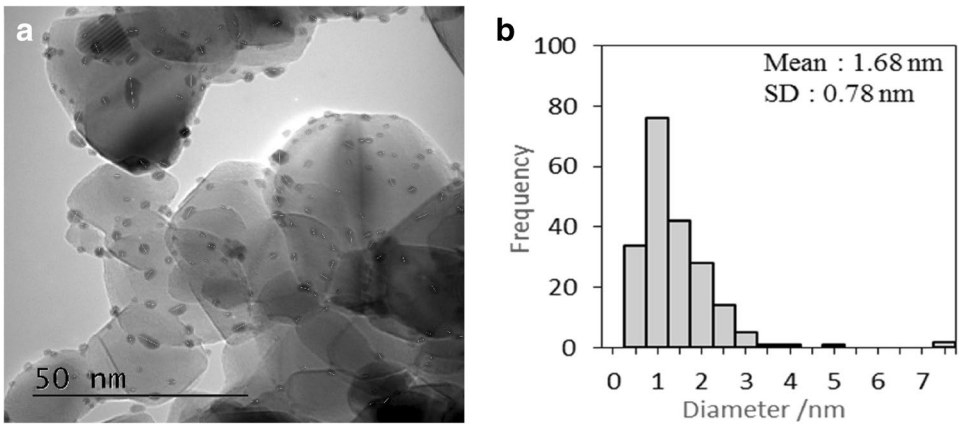

Fig. 1 Representative Transmission electron microscopy of $AuPt/LaTiO_2$ (**a**) and associated particle size distribution (**b**)

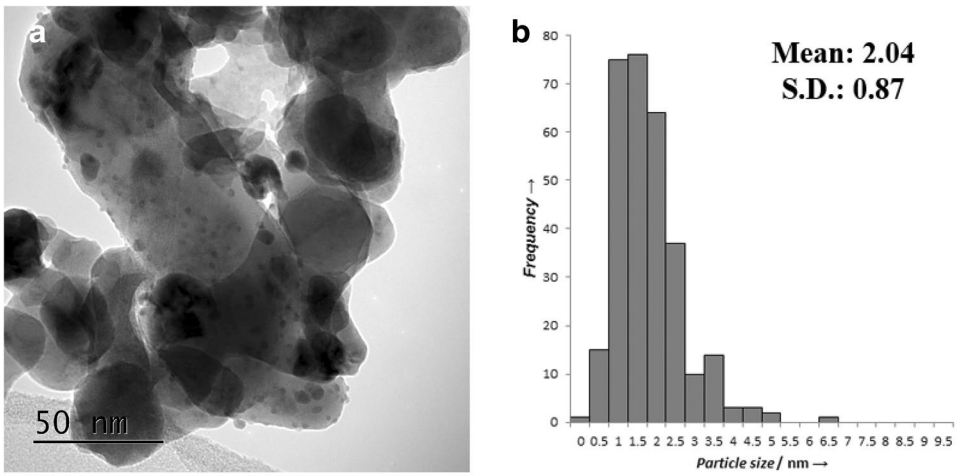

Fig. 2 Representative Transmission electron microscopy of $AuPt/LaMnO_3$ (**a**) and associated particle size distribution (**b**)

only catalysts deactivating and Au-Pt ones being stable, when these catalysts were studied for the purposeful production of lactic acid and attributed this to a change in metal-support interaction [15].

Taking these observations into account, the effect of Au:Pt ratio on catalytic performance was investigated with a SAS prepared $LaMnO_3$ support. Figure 4 shows time online analysis of these catalysts for the glycerol oxidation reaction, with TOFs and product breakdown compared to the TiO_2 catalysts given in Table 2. Firstly, a general improvement in initial TOF for all metal compositions can be observed for $LaMnO_3$ supported catalysts, relative to TiO_2 supported catalysts. Of particular note is the significant improvement in the TOF of the Au only catalyst between the two supports, with $Au/LaMnO_3$ have a TOF of 370 h^{-1} vs that of 220 h^{-1} for Au/TiO_3. As seen with Au/TiO_3, the rate of glycerol conversion using $Au/LaMnO_3$ notably decreased with time online, however to a less significant extent to Au/TiO_2. Strong metal-support reactions have previously been reported for $Au/LaMnO_3$ catalysts during gas phase oxidations, which potentially explains the difference in stability for this catalyst vs Au/TiO_2 [25].

The stability of $LaMnO_3$ catalysts to leaching, under these reactions has been previously reported [14, 22]. Consultation of the relevant Pourbaix diagram (Fig. 4) shows that in the absence of the NaOH, $LaMnO_3$ is highly prone to dissolution from acid products [22]. However, the addition of NaOH maintains a pH of > 12 (even in the event of 100% conversion to formic acid) under which the support is stable, as evidenced by only 60 ppm La and 20 ppm Mn being observed over a 2 h catalyst cycle [14]. Elemental analysis has shown there to be no observable Au or Pt leaching during reaction.

In contrast to the TiO_2 supported catalysts, all $LaMnO_3$ catalysts (regardless of Au/Pt composition) had low yield (below 10%) towards lactic acid. This finding agreed with our previous observations of low lactic acid selectivity for lanthanum perovskite supports with high oxygen absorption capacity ($LaMnO_3$ and $LaCoO_3$) and high lactic acid selectivity with perovskites exhibiting low oxygen absorption capacity ($LaCrO_3$, $LaFeO_3$ and $LaNiO_3$) [14]. The employment of only AuPt nanoparticles in the previous study raised the question as to whether the effect of the support was to modify the AuPt morphology, which then effected selectivity towards oxidation or dehydration products. Clearly, the

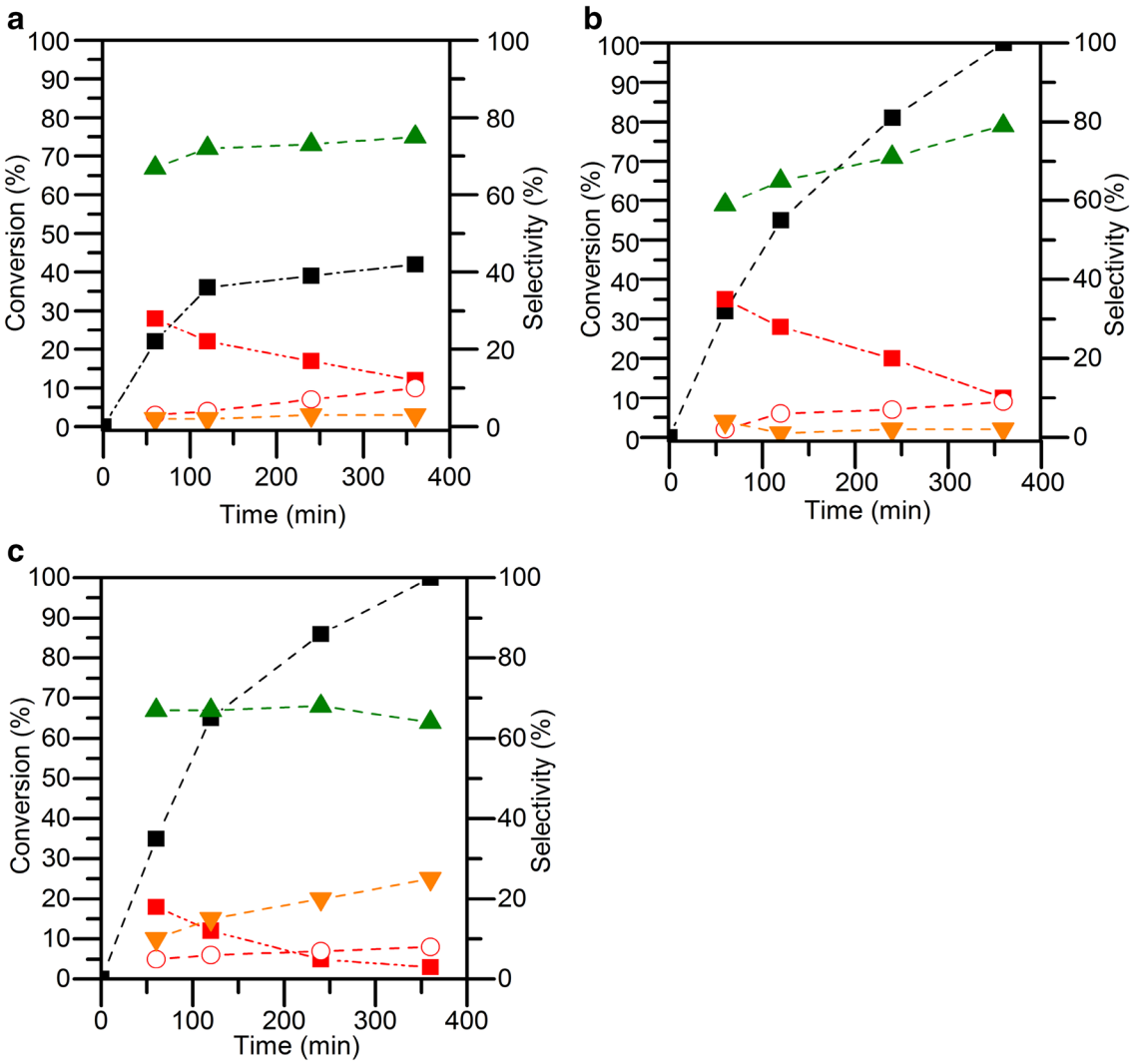

Fig. 3 Time online glycerol oxidation of 1wt% Au, Pt or AuPt/TiO_2 catalysts **a** Au/TiO_2; **b** AuPt/TiO_2, **c** Pt/TiO_2. Key for (**a**–**c**); glycerol conversion (■); selectivity to glyceric acid (■), tartronic acid (○), lactic acid (▲) and C–C scission products (▼). Carbon mass balances between 95 and 105%. Reaction conditions: 100 °C, 3 bar O_2, 4:1 NaOH:glycerol (molar), 1000:1 gylcerol:metal (molar)

Table 2 Catalytic performance during glycerol oxidation

Catalyst	TON[a]	TOF[b] (h^{-1})	Yield at 6 h (%)		
			Glyceric acid	Tartronic acid	Lactic acid
Au/TiO_2	420	220	5.0	4.2	31.5
AuPt/TiO_2	1000	320	6.6	4.2	31.5
Pt/TiO_2	1000	350	3.0	8.0	63.9
Au/$LaMnO_3$	620	370	14.9	44.0	0.0
AuPt/$LaMnO_3$	750	390	52.5	13.5	3.8
Pt/$LaMnO_3$	780	330	20.3	10.9	1.6

[a]Moles glycerol converted per mole of metal,

[b]Moles glycerol converted per mole of metal per h, taken at 1 h of reaction. Reaction conditions: 100 °C, 3 bar O_2, 4:1 NaOH:glycerol (molar), 1000:1 gylcerol:metal (molar)

low lactic acid selectivity for both the Au/$LaMnO_3$ and Pt/$LaMnO_3$ catalysts, shown in Fig. 5, demonstrated that the support itself controls/inhibits dehydration and the lactic acid reaction pathway and not the nanoparticle composition.

The inhibition of the dehydration pathway is quite remarkable, given that it has been demonstrated that initial glycerol oxidation products of glyceraldehyde and 1,3,dihydroxyacetone have been shown to readily undergo dehydration and rearrangement to lactic acid in the presence of base alone (i.e. with an absence of a catalyst) [13]. Specifically, lactic acid selectivity is dictated by a reaction step that occurs in solution. If a carboxylic acid has been produced from the oxidation of these shared intermediates (with dehydration pathway), lactic acid cannot form (see scheme 1). Therefore, inhibition of the dehydration reaction by the $LaMnO_3$ support can be attributable to a significantly

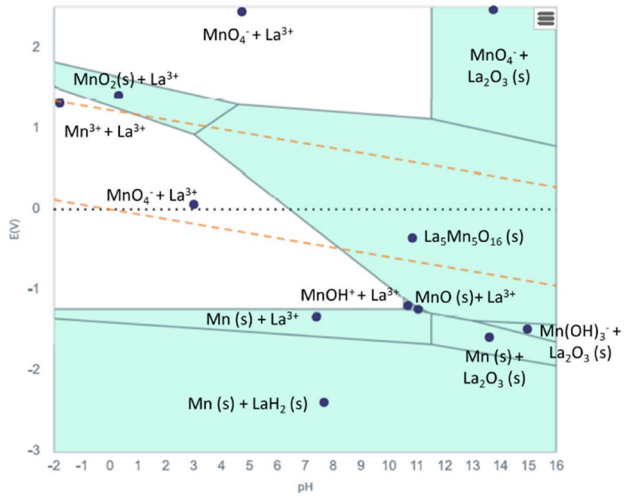

Fig. 4 Pourbaix diagram for La,Mn,O system. Representative diagram generated using the Materials Project [27]. Green represents solid phases and white solvated. Dashed lines are the stable region for water

reduced desorption of glycerol oxidation intermediates during their sequential oxidation.

While $LaMnO_3$ supresses lactic acid, product selectivity associated with the oxidation reaction pathway is affected by the metal composition. As observed with TiO_2 supported catalysts, Au prevents C–C scission, with both $Au/LaMnO_3$ and $AuPt/LaMnO_3$ catalysts exhibiting less than 10% selectivity towards scission products; while the reaction with the $Pt/LaMnO_3$ catalyst had high C–C scission product selectivity that exceeded 50% over the reaction. The significantly higher C–C scission selectivity for the $Pt/LaMnO_3$ compared to Pt/TiO_2 (C–C scission after 6 h of 58% selectivity and 25% selectivity respectively) can be attributed to the prevalence of the dehydration reaction in the latter catalyst.

Another notable effect regarding metal composition is the extent of the sequential oxidation of glycerol to tartronic acid (via glyceric acid). Yields of tartroic acid with reaction time on-line are shown in Fig. 6, and final product yield after 6 h are given in Table 2. Due to the high C–C scission rate, very little tartronic acid was formed using the $Pt/LaMnO_3$ catalyst during the reaction. The $AuPt/LaMnO_3$ catalyst resulted in high glyceric acid selectivity over the 6 h time on line, with a slight increase in tartronic acid formation towards the end of the reaction to give a final yield of 13.5%. The secondary oxidation of glyceric acid to tartronic acid appears to be suppressed while significant glycerol substrate remains present in the reaction. However, low C–C scission and lactic acid formation over the 6 h reaction shows that tartronic acid formation could be achieved by extending the reaction time, as demonstrated by the complete conversion of all glycerol and glyceric acid to give 87% tartronic acid yield over 24 h reaction time. Interestingly, the $Au/LaMnO_3$ catalyst has high activity for the conversion of glyceric acid into tartronic acid, with a yield of 44% at 6 h reaction time, while glycerol was still present in the reaction mixture. After 24 h this catalyst gave an exceptional 92% selectivity towards tartronic acid, yet even after this time-period, glycerol conversion was only 87%, giving a final tartronic acid yield of 80%.

As noted, Au only catalysts showed a marked decrease in glycerol conversion with time (vide supra), yet it seems that further oxidation of glyceric acid occurs after glycerol oxidation has stopped or markedly slowed. Conformation of this can seen from simple plots of reactant and product concentrations with time on-line (Fig. 7). A reaction with $AuPt/LaMnO_3$ shows a clear increase in glycerol acid concentration as that of glycerol drops which, as previously reported, reaches a maximum concentration once all glycerol has been consumed, before itself being consumed to produce tartronic acid. In the case of reactions using $Pt/LaMnO_3$, glyceric acid concentration remains at steady state from 60 to 360 min, while glycerol continues to be consumed to produce C–C scission products and small quantities of tartronic acid. Most interestingly, glyceric acid concentration peaks within the 1st h of reaction when using the $Au/LaMnO_3$ catalyst and then steadily decreases, even while the rate of glycerol consumption slows dramatically. Tartronic acid is formed at a steady rate throughout the 6 h reaction period, suggesting that oxidation of glyceric acid to tartronic acid is preferred over glycerol oxidation. As glycerol conversion almost stops at 6 h but tartronic acid formation and glyceric acid consumption continue, there must be different reaction pathways and/or different catalytically active sites for these two reactions on the Au catalysed surface.

Freakley, Hutchings and co-workers showed that selectivity towards glyceric or tartronic acid could be influenced by the amount of polymeric stabiliser used in Au nano particle synthesis. High tartronic acid selectivity being observed when little or no stabiliser was used, while high glyceric acid yields were reported when higher concentrations of stabiliser were used [26]. A potential cause of the switch between a glycerol oxidation pathway and a glyceric acid oxidation pathway seen in $Au/LaMnO_3$ could be that the surface coverage of the PVA stabilising polymer decreased during the reaction, which is expected under aqueous reaction media at elevated temperatures. Alternatively, specific active sites for glycerol oxidation were blocked by product inhibition during the reaction.

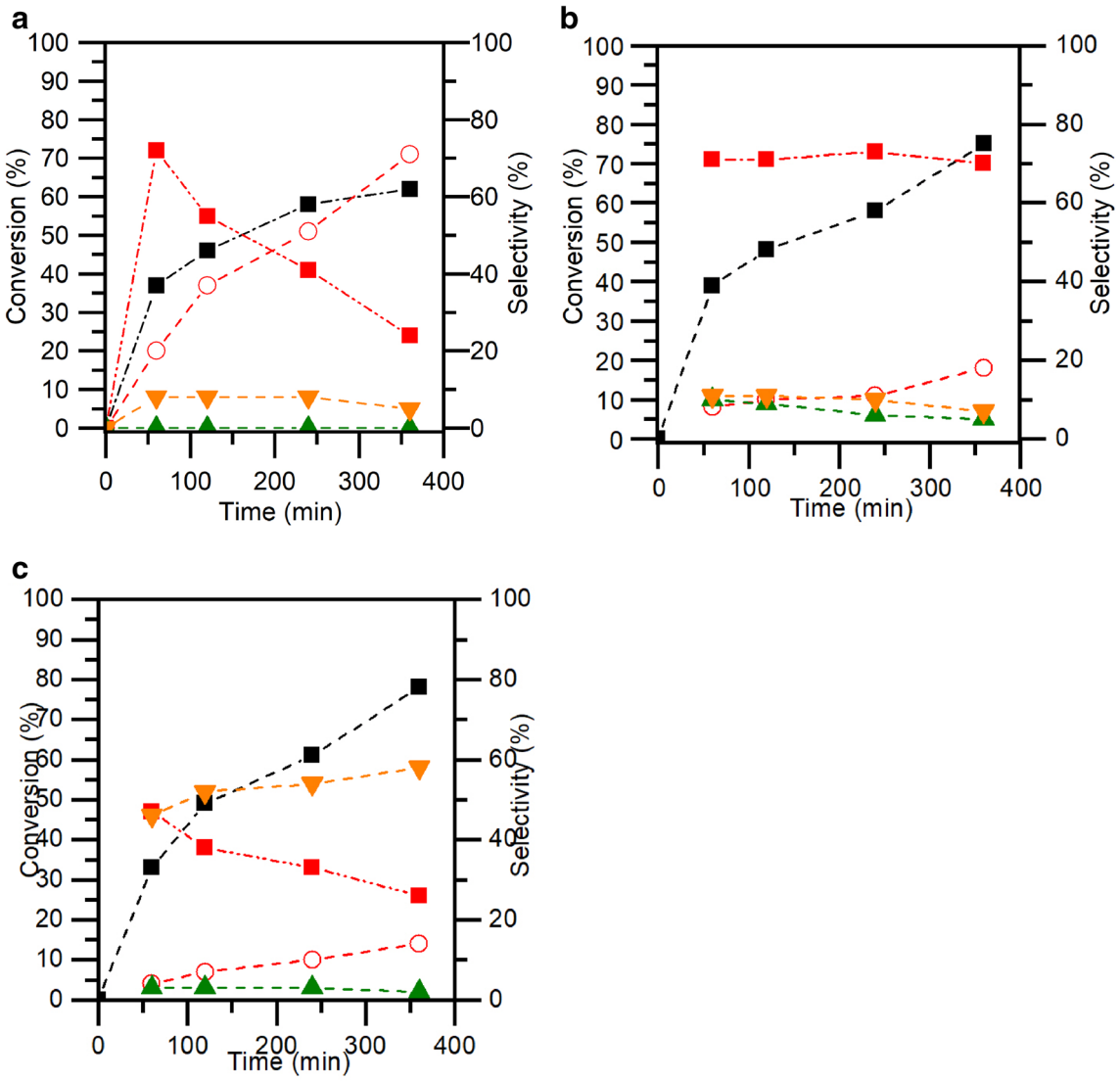

Fig. 5 Time online glycerol oxidation of 1wt% $Au_xPt_y/LaMnO_3$ catalysts with varied Au/Pt molar composition. **a** $Au/LaMnO_3$, **b** $Au_1Pt_1/LaMnO_3$, **c** $Pt/LaMnO_3$; Key for (**a**–**c**); glycerol conversion (■); selectivity to glyceric acid (■), tartronic acid (○), lactic acid (▲) and C–C scission products (▼). Carbon mass balances between 95 and 105%. Reaction conditions: 100 °C, 3 bar O_2, 4:1 NaOH:glycerol (molar), 1000:1 gylcerol:metal (molar)

4 Conclusion

Using reaction conditions to favour sequential oxidation of glycerol to produce tartronic acid, i.e. temperatures of 100 °C and a 4:1 NaOH: glycerol ratio, has limited effect when using conventional TiO_2 supported Au, AuPt or Pt nanoparticle catalysts. The reason for this being the preference for the dehydration and structural rearrangement of initial aldehyde products to form lactic acid. This lactic acid reaction pathway is switched off when a $LaMnO_3$ support is used, irrespective of the choice of metal nanoparticle, i.e. monometallic Au or Pt, or bimetallic catalysts produce none or minimal lactic acid over 6 h reaction. It is therefore clear that the support structure is responsible for shutting down the dehydration pathway. Choice of nanoparticle composition did however influence reaction selectivity, with Pt alone facilitating C–C scission and alloying with Au supressing these reactions to favour glyceric acid production. Au only catalysts demonstrated interesting behaviour under the reaction conditions used; firstly, Au only catalysts had comparable turn over frequencies to AuPt alloyed catalysts. Secondly, while the catalysis of glycerol oxidation underwent rapid

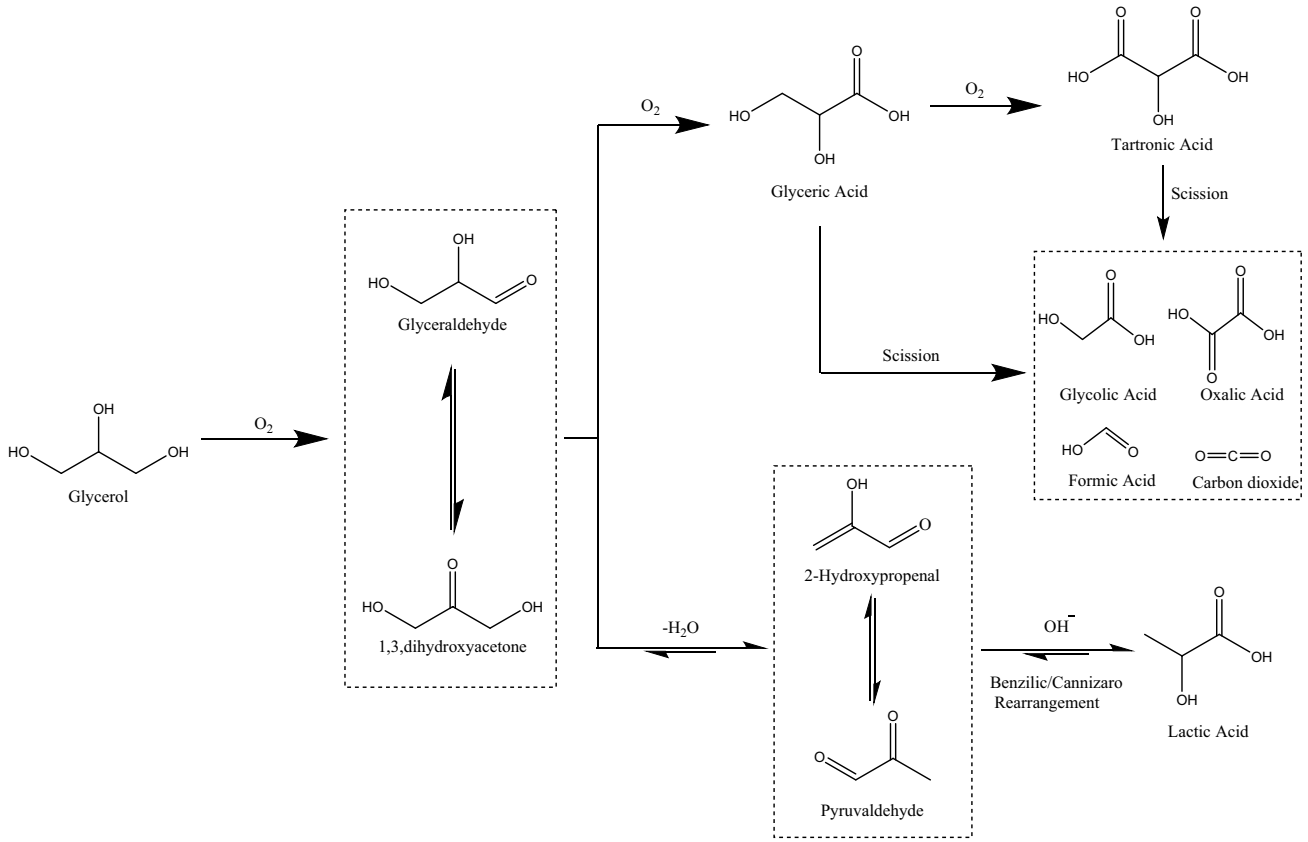

Scheme 1 Possible reaction pathways for glycerol oxidation

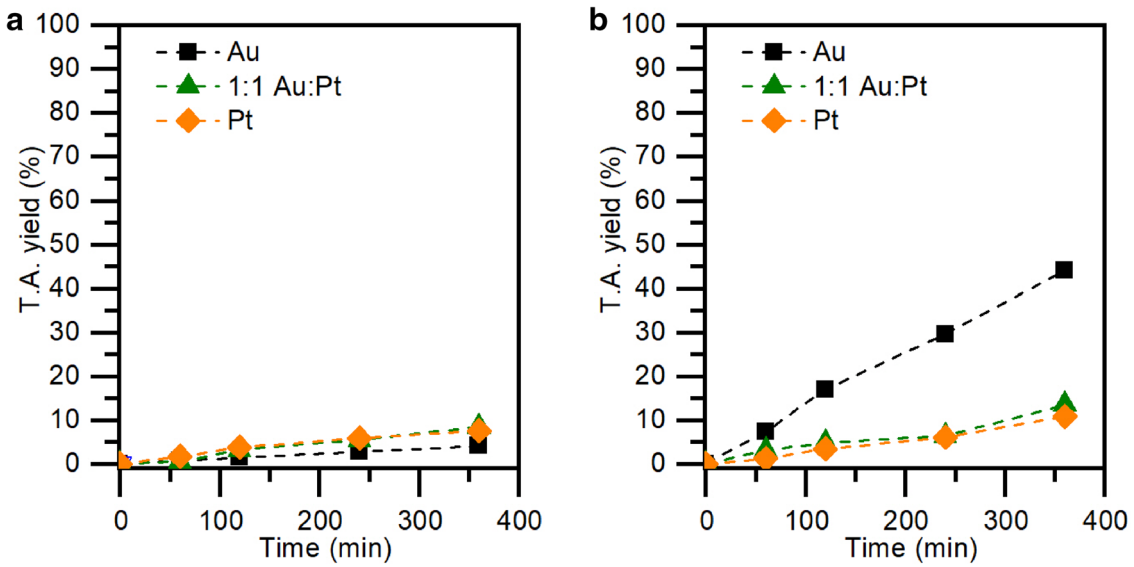

Fig. 6 Time online tartronic acid yield with varied Au/Pt molar composition catalysts. **a** TiO_2 supported catalysts. **b** $LaMnO_3$ supported catalysts. Reaction conditions: 100 °C, 3 bar O_2, 4:1 NaOH:glycerol (molar), 1000:1 gylcerol:metal (molar)

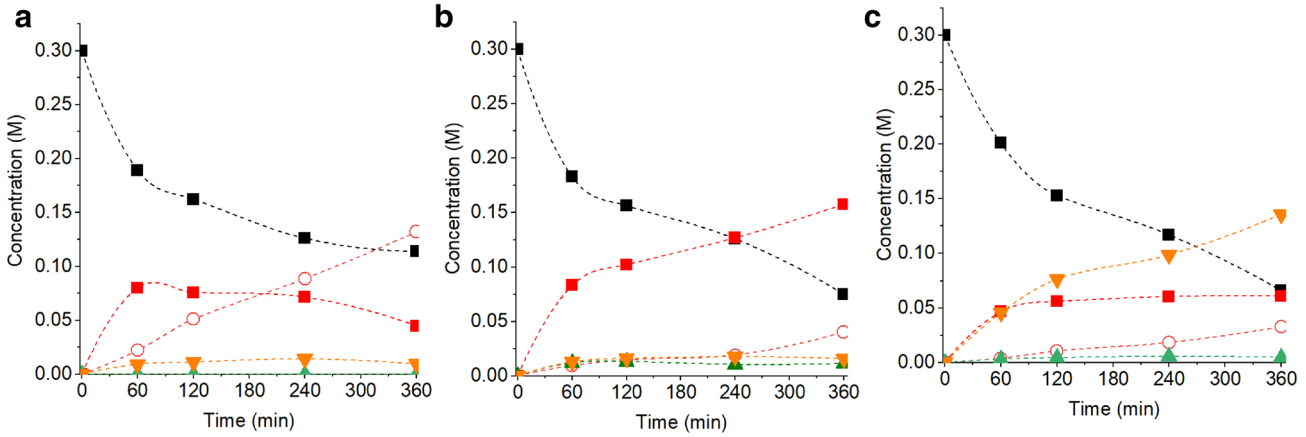

Fig. 7 Concentration of reactants and products during glycerol oxidation using $LaMnO_3$ supported catalysts. **a** Reaction using Au/$LaMnO_3$; **b** Reaction using AuPt/$LaMnO_3$; **c** Reaction using Pt/$LaMnO_3$. Key: Glycerol (■); glyceric acid(■); tartronic acid(○); C–C products(▼); lactic acid(▲)

deactivation, the sequential oxidation of glyceric acid to tartronic acid was relatively unaffected. Such an observation was only possible due to the lactic acid pathway being suppressed by the $LaMnO_3$ support.

Acknowledgements UK Catalysis Hub is kindly thanked for resources and support provided via our membership of the UK Catalysis Hub Consortium and funded by EPSRC grant: EP/R026939/1, EP/R026815/1, EP/R026645/1, EP/R027129/1.

References

1. Corma A, Iborra S, Velty A (2007) Chemical routes for the transformation of biomass into chemicals. Chem Rev 107:2411–2502. https://doi.org/10.1021/cr050989d
2. Gallezot P (2012) Conversion of biomass to selected chemical products. Chem Soc Rev 41:1538–1558. https://doi.org/10.1039/C1CS15147A
3. Prati L, Rossi M (1998) Gold on carbon as a new catalyst for selective liquid phase oxidation of diols. J Catal 176:552–560. https://doi.org/10.1006/jcat.1998.2078
4. Carrettin S, McMorn P, Johnston P et al (2002) Selective oxidation of glycerol to glyceric acid using a gold catalyst in aqueous sodium hydroxide. Chem Commun. https://doi.org/10.1039/B201112N
5. Garcia R, Besson M, Gallezot P (1995) Chemoselective catalytic oxidation of glycerol with air on platinum metals. Appl Catal A: Gen 127:165–176. https://doi.org/10.1016/0926-860X(95)00048-8
6. Dimitratos N, Porta F, Prati L (2005) Au, Pd (mono and bimetallic) catalysts supported on graphite using the immobilisation method: synthesis and catalytic testing for liquid phase oxidation of glycerol. Appl Catal A: Gen 291:210–214. https://doi.org/10.1016/j.apcata.2005.01.044
7. Bianchi CL, Canton P, Dimitratos N et al (2005) Selective oxidation of glycerol with oxygen using mono and bimetallic catalysts based on Au, Pd and Pt metals. Catal Today 102–103:203–212. https://doi.org/10.1016/j.cattod.2005.02.003
8. Villa A, Campione C, Prati L (2007) Bimetallic gold/palladium catalysts for the selective liquid phase oxidation of glycerol. Catal Lett 115:133–136. https://doi.org/10.1007/s10562-007-9077-x
9. Villa A, Campisi S, Chan-Thaw CE et al (2015) Bismuth modified Au-Pt bimetallic catalysts for dihydroxyacetone production. Catal Today 249:103–108. https://doi.org/10.1016/j.cattod.2014.12.012
10. Brett GL, He Q, Hammond C et al (2011) Selective oxidation of glycerol by highly active bimetallic catalysts at ambient temperature under base-free conditions. Angew Chem Int Ed 50:10136–10139. https://doi.org/10.1002/anie.201101772
11. Villa A, Dimitratos N, Chan-Thaw CE et al (2015) Glycerol oxidation using gold-containing catalysts. Acc Chem Res 48:1403–1412. https://doi.org/10.1021/ar500426g
12. Purushothaman RKP, van Haveren J, van Es DS et al (2014) An efficient one pot conversion of glycerol to lactic acid using bimetallic gold-platinum catalysts on a nanocrystalline CeO2 support. Appl Catal B: Environ 147:92–100. https://doi.org/10.1016/j.apcatb.2013.07.068
13. Evans CD, Douthwaite M, Carter JH et al (2020) Enhancing the understanding of the glycerol to lactic acid reaction mechanism over AuPt/TiO2 under alkaline conditions. J Chem Phys 152:134705. https://doi.org/10.1063/1.5128595
14. Evans CD, Kondrat SA, Smith PJ et al (2016) The preparation of large surface area lanthanum based perovskite supports for AuPt nanoparticles: tuning the glycerol oxidation reaction pathway by switching the perovskite B site. Faraday Discuss 188:427–450. https://doi.org/10.1039/C5FD00187K
15. Shen Y, Zhang S, Li H et al (2010) Efficient synthesis of lactic acid by aerobic oxidation of glycerol on Au–Pt/TiO2 catalysts.

Chem—A Eur J 16:7368–7371. https://doi.org/10.1002/chem.201000740
16. Cai J, Ma H, Zhang J et al (2014) Catalytic oxidation of glycerol to tartronic acid over Au/HY catalyst under mild conditions. Chin J Catal 35:1653–1660. https://doi.org/10.1016/S1872-2067(14)60132-7
17. Rodriguez AA, Williams CT, Monnier JR (2014) Selective liquid-phase oxidation of glycerol over Au–Pd/C bimetallic catalysts prepared by electroless deposition. Appl Catal A: Gen 475:161–168. https://doi.org/10.1016/j.apcata.2014.01.011
18. Jin X, Zhao M, Zeng C et al (2016) Oxidation of glycerol to dicarboxylic acids using cobalt catalysts. ACS Catal 6:4576–4583. https://doi.org/10.1021/acscatal.6b00961
19. Carrettin S, McMorn P, Johnston P et al (2003) Oxidation of glycerol using supported Pt, Pd and Au catalysts. Phys Chem Chem Phys 5:1329–1336. https://doi.org/10.1039/B212047J
20. Tsuji A, Rao KTV, Nishimura S et al (2011) Selective oxidation of glycerol by using a hydrotalcite-supported platinum catalyst under atmospheric oxygen pressure in water. ChemSusChem 4:542–548. https://doi.org/10.1002/cssc.201000359
21. Villa A, Campisi S, Mohammed KMH et al (2015) Tailoring the selectivity of glycerol oxidation by tuning the acid–base properties of Au catalysts. Catal Sci Technol 5:1126–1132. https://doi.org/10.1039/C4CY01246A
22. Inns DR, Mayer AJ, Skukauskas V et al (2021) Evaluating the activity and stability of perovskite LaMO3-based Pt catalysts in the aqueous phase reforming of glycerol. Top Catal 64:992–1009. https://doi.org/10.1007/s11244-021-01449-6
23. Kremenić G, Nieto JML, Tascón JMD, Tejuca LG (1985) Chemisorption and catalysis on LaMO3 oxides. J Chem Soc Faraday Trans 1 Phys Chem Condens Ph 81:939–949. https://doi.org/10.1039/F19858100939
24. Kondrat SA, Smith PJ, Wells PP et al (2016) Stable amorphous georgeite as a precursor to a high-activity catalyst. Nature 531:83–87. https://doi.org/10.1038/nature16935
25. Liu Y, Dai H, Deng J et al (2013) PMMA-templating generation and high catalytic performance of chain-like ordered macroporous LaMnO3 supported gold nanocatalysts for the oxidation of carbon monoxide and toluene. Appl Catal B: Environ 140–141:317–326. https://doi.org/10.1016/j.apcatb.2013.04.025
26. Abis L, Dimitritatos N, Sankar M et al (2020) The effect of polymer addition on base catalysed glycerol oxidation using gold and gold-palladium bimetallic catalysts. Top Catal 63:394–402. https://doi.org/10.1007/s11244-019-01212-y
27. Patel AM, Nørskov JK, Persson KA, Montoya JH (2019) Efficient Pourbaix diagrams of many-element compounds. Phys Chem Chem Phys 21:25323–25327. https://doi.org/10.1039/C9CP04799A